

# Inter-decadal changes in the East Asian summer monsoon and associations with sea surface temperature anomaly in the South Indian Ocean

Haiyan Zhang<sup>1</sup> · Zhiping Wen<sup>1,4</sup> · Renguang Wu<sup>2</sup> · Zesheng Chen<sup>3</sup> · Yuanyuan Guo<sup>1</sup>

Received: 8 September 2015 / Accepted: 13 April 2016 / Published online: 20 April 2016  
© Springer-Verlag Berlin Heidelberg 2016

**Abstract** Previous studies have revealed inter-decadal changes in the East Asian summer monsoon (EASM) that occurred around the late 1970s and early 1990s, respectively. The present study compares characteristics of these two changes and analyzes plausible influences of the South Indian Ocean (SIO) sea surface temperature (SST) change. The two changes share pronounced common features, characterized by an equivalent barotropic circulation anomaly over northern East Asia and a meridional vertical overturning circulation over the tropical region. Meanwhile, they display some distinct characteristics, especially over the tropics. The circumfluent anomalies are more robust for the first change than for the second one. Related amplitude asymmetry is partly attributed to a weakening trend in the EASM. Moreover, SST change in the SIO, featuring a decadal warming since the 1980s and a cooling after 1993, may contribute to both of these inter-decadal changes. Cold SST anomaly induces anomalous mid-tropospheric descent over the western SIO and ascent extending from the eastern SIO to western Australia and over the equatorial Indian Ocean. The accompanying upper-tropospheric divergent

flows from western Australia and equatorial Indian Ocean to the Philippines lead to anomalous descent and an anomalous lower-tropospheric anticyclone over the South China Sea–Philippines. Warm SST anomaly induces opposite changes in above regions. The possible influence of SST anomaly in the SIO is further confirmed by numerical experiments.

**Keywords** Inter-decadal changes · East Asian summer monsoon · SST anomaly in the South Indian Ocean

## 1 Introduction

As an integral part of the Asian climate system, the East Asian summer monsoon (EASM) is quite unique and has a complex spatio-temporal structure that encompasses tropics, subtropics, and mid-latitudes. Climate disasters that arise from monsoon circulation and precipitation anomalies exert strong impacts on the regional agriculture, water resources, economy, and society. Of great scientific importance is the prominent variability of the EASM on intraseasonal to inter-decadal timescales. One dominating mode of intraseasonal variability of summer circulation and precipitation over East Asia is the 30–60-day oscillation, the other one is the 10–20-day oscillation (Chen and Xie 1988; Mao and Chan 2005; Ju et al. 2005; Guan and Johnny 2006). On the inter-annual time scale, the quasi-2-yr and quasi-4-yr oscillations are highlighted (Chen et al. 1990; Wu et al. 2008), which are closely related to the mechanism of the warm ocean–atmosphere interaction and the El Niño–Southern Oscillation (ENSO) impact (Chen et al. 1989; Meehl and Arblaster 2002; Li et al. 2006).

In recent years, inter-decadal variability of the EASM has drawn great attention. A significant climate shift

✉ Zhiping Wen  
eeswzp@mail.sysu.edu.cn

<sup>1</sup> Center for Monsoon and Environment Research and School of Atmospheric Sciences, Sun Yat-Sen University, Guangzhou 510275, China

<sup>2</sup> Center for Monsoon System Research, Institute of Atmospheric Physics, Chinese Academy of Sciences, Beijing 100080, China

<sup>3</sup> State Key Laboratory of Tropical Oceanography, South China Sea Institute of Oceanology, Chinese Academy of Sciences, Guangzhou, China

<sup>4</sup> Jiangsu Collaborative Innovation Center for Climate Change, Nanjing, China

occurred around the late 1970s, featuring an increase in summer rainfall over the Yangtze River region and a decrease in rainfall over South China and North China (Nitta and Hu 1996; Wu and Chen 1998; Zhai et al. 2005; Ding et al. 2008). Coherent changes in atmospheric circulation have been identified, including a significant weakening of the tropical upper-level easterly jet, southward displacement of the East Asian subtropical westerly jet (EASWJ) and westward extension of the western Pacific subtropical high (WNPSH) (Yu et al. 2004; Ding et al. 2008; Zhou et al. 2009). Intensity of the EASM weakened abruptly at the same time (Wang 2001; Guo et al. 2003). The shift in summer monsoon concurred with large-scale inter-decadal variations in sea and land surface thermal conditions around the end of 1970s (Nitta and Yamada 1989; Trenberth and Hurrell 1994; Ding et al. 2009). It was proposed that the sea surface temperature (SST) forcing, primarily in the tropical regions, was able to induce most of the observed weakening of the EASM (Li et al. 2010). Influences of the Pacific decadal oscillation (PDO) or the Interdecadal Pacific Oscillation (IPO), and Indian Ocean–western Pacific (IWP) SST warming were emphasized. For instance, Ding et al. (2009) manifested that inter-decadal warming of the SST in the tropical central and eastern Pacific reduced the land–sea thermal contrast in summer in the Asian monsoon region, which further led to weakening of monsoon. Zhou et al. (2009) suggested that the observed IWP warming can partly account for the westward extension of the WNPSH through analyses of model simulations. Several studies have also suggested contributions of the Tibetan Plateau snow and the Arctic sea ice concentration to the climate change (Ding et al. 2009; Wu et al. 2009).

In addition to the well-known climate change in the late 1970s, a decadal change in the early 1990s over East Asia was revealed. On the inter-decadal scale, the precipitation variability mode changed from a typical tripole to a dipole structure, which brought a notable increase in summer rainfall over South China (Ding et al. 2008; Liu et al. 2011). Kwon et al. (2007) suspected that a remarkable increase in the number of the typhoon passing through the southeastern part of China may be partly responsible for the decadal increase in precipitation over the same area. Wu et al. (2010) argued that SST warming in the equatorial Indian Ocean (IO) and an increase in the Tibetan Plateau snow cover in the preceding winter–spring can induce two anomalous anticyclones at the lower level: one over the South China Sea (SCS)–subtropical western North Pacific (WNP), and the other over north China–Mongolia, which further lead to anomalous moisture convergence, enhanced ascent, and increased rainfall over South China. Zhu et al. (2013) found that Meiyu rainfall over the Yangtze–Huaihe River valley experienced a decadal change around the beginning of 1990s with a seesaw-like distribution.

Coherently, the EASM has undergone a decadal change around 1993 (Kwon et al. 2007; Zhu et al. 2014). The decadal change was characterized by a distinctive decrease in the strength of zonal winds near the subtropical jet over East Asia, which was understood as a barotropic response to a forcing associated with heating from increased precipitation over South China. Meanwhile, the major modes of variations of summer precipitation over the East Asia and the relationships between the EASM and WNP summer monsoon, ENSO, SST in the North Atlantic have experienced significant decadal changes around the 1990s (Kwon et al. 2005; Yim et al. 2008, 2014). Besides, a significant advance in the onset dates of the SCS summer monsoon around 1993/4 was detected. Related roles of SST anomalies in the tropics have been discussed (Kajikawa and Wang 2012; Yuan and Chen 2013; Xiang and Wang 2013).

Most of the previous studies investigated the climate changes that occurred in the late 1970s and early 1990s separately because of their distinct characteristics and influences. Are there any common features between them? By a simple comparison, we notice that features of these inter-decadal changes in the EASM are similar to a great extent, except that their signs of anomalies are opposite and that amplitudes of signals over the tropics are asymmetric (Fig. 3). What may be responsible for the intercommunity? How to interpret the amplitude asymmetry? SST forcing is thought to be one of the most important factors that can affect variability of monsoon system on multiple time scales. Is there any SST forcing that may be responsible for both the late 1970s change and the early 1990s change? This study attempts to answer these questions.

The rest of the paper is organized as follows. The datasets, analysis methods and model used in the present study are described in Sect. 2. Section 3 presents variability of the entire EASM system on longer time scales as a background. In Sect. 4, we focus on substantial inter-decadal changes in the EASM that occur in the late 1970s and early 1990s, respectively. Both their common features and differences will be discussed. Section 5 suggests possible roles of SST anomalies in the South Indian Ocean (SIO) on these decadal changes. Finally, the summary and discussion are given in Sect. 6.

## 2 Data, methodology and model

The primary data used in the present analysis are derived from the Japan Meteorological Agency (JMA) 55-year Reanalysis (JRA-55, Kobayashi et al. 2015) for the period 1958–2012, which includes summer (June–July–August) monthly mean winds at 850 and 200 hPa, vertical velocity at 500 hPa, geopotential heights at 850 and 200 hPa, and velocity potential at 850 and 200 hPa. There may be

unrealistic inter-decadal variability in the National Centers for Environmental Prediction–National Center for Atmospheric Research (NCEP–NCAR) reanalysis (Yang et al. 2002; Wu et al. 2005). Thus, the 40-year European Centre for Medium-Range Weather Forecasts (ECMWF) Reanalysis (ERA-40, Uppala et al. 2005) for the period 1958–2002 is used to validate primary results based on JRA-55 data. These two reanalysis use different spatial resolutions: JRA-55 has  $1.25^\circ \times 1.25^\circ$  resolution, and ERA-40 has  $2.5^\circ \times 2.5^\circ$  resolution. Precipitation data used is the monthly mean precipitation from the Climatic Research Unit (CRU; New et al. 2000), with a spatial resolution of  $1^\circ \times 1^\circ$ , covering the period from January 1958 to December 2012. The present study uses monthly SST from the Hadley Centre of the UK Met Office (HadISST, Rayner et al. 2003). The SST is available on a  $1^\circ \times 1^\circ$  grid starting from January 1847.

A multivariate empirical orthogonal function (MV-EOF) analysis is performed on a set of four meteorological fields in June–August (JJA), including 850 and 200-hPa winds over East China to derive the leading modes of variability of EASM circulation. The MV-EOF analysis method was described in detail in Wang (1992). A linear regression analysis is employed to extract components corresponding to each leading mode from total fields, to discuss the relative contributions of MV-EOF2 and MV-EOF3 to the late 1970s change and the early 1990s change, respectively. In order to analyze the possible influences of natural decadal variability of SST on the EASM, the present study applies a harmonic analysis to SST and wind fields, separating inter-decadal component from inter-annual component whose period is shorter than 9 years. By taking into account the effect of the filtering on the degree of freedom and significance test, the effective degrees of freedom are evaluated (Chen 1982). A composite analysis and the Student's *t* test are also used.

The present study use the National Center for Atmospheric Research (NCAR) Community Atmospheric Model version 4.0 (CAM4, Neale et al. 2013) to confirm the possible influence of SST forcing in the SIO on inter-decadal variation of the EASM. The model horizontal resolution is about  $2.5^\circ$  longitude by  $1.9^\circ$  latitude and 26 vertical-levels. We conduct two experiments using CAM4 model. In the control experiment, the model is integrated for 20 years using the climatological mean seasonal cycle of SST. Parallel to the control experiment, a sensitivity experiment is performed with imposed JJA SST anomaly of  $-0.3^\circ\text{C}$  in the region of  $20^\circ\text{--}40^\circ\text{S}$  and  $45^\circ\text{--}90^\circ\text{E}$ .

### 3 Variability of the EASM system on longer time scales

To illustrate the spatial and temporal structures of the EASM, a MV-EOF analysis of the 850 and 200-hPa winds

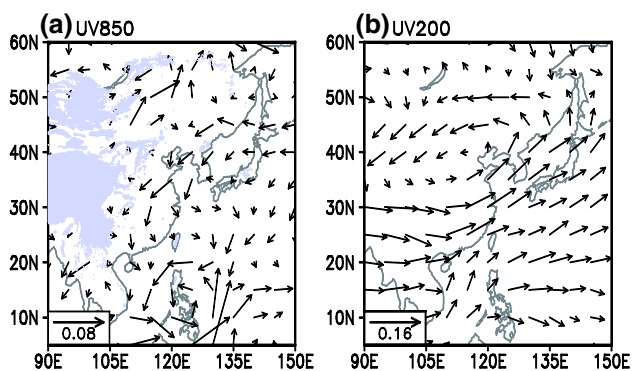
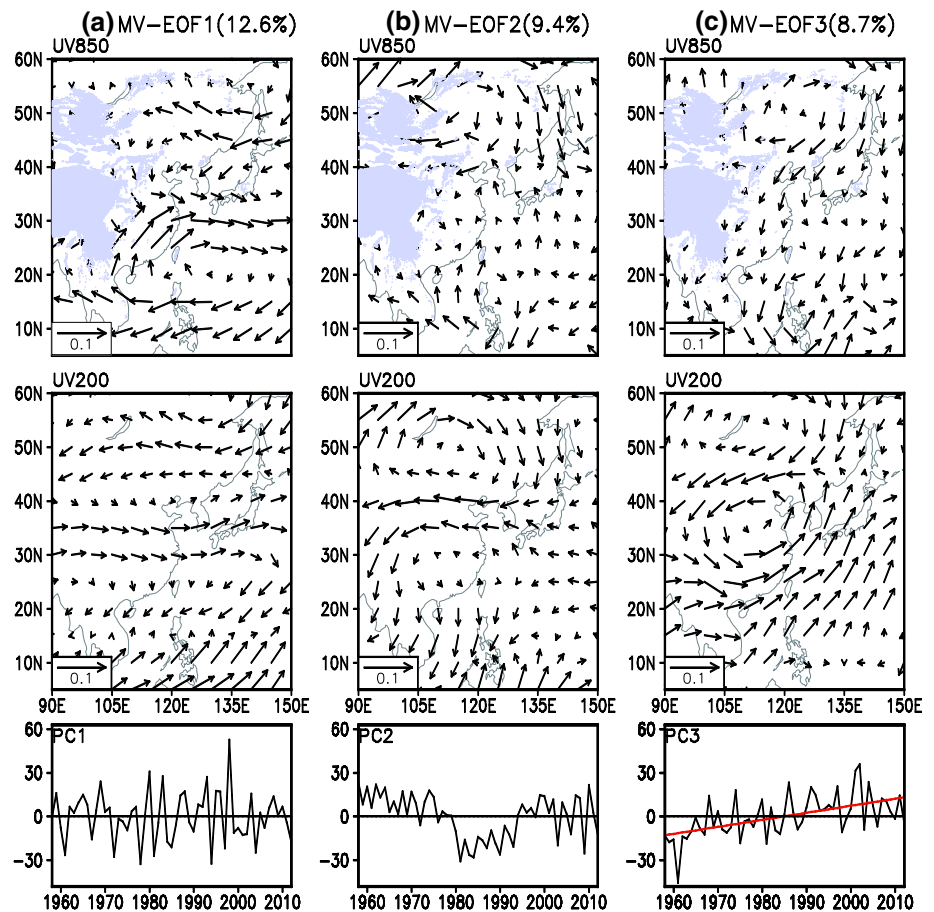
over the East Asian domain ( $5^\circ\text{--}60^\circ\text{N}$ ,  $90^\circ\text{--}150^\circ\text{E}$ ) is conducted because of its distinct three-dimensional structure. The analysis is suitable for study of inter-decadal variations due to that circulation data are more reliable and have longer records than precipitation data. The first three MV-EOF modes carry about 30.7 % of the total variance, which account for 12.6, 9.4 and 8.7 %, respectively. According to the rule by North et al. (1982), the first leading mode is statistically distinguished from higher modes. The second mode is not totally separated from the third one. The statistical inseparability of these two modes may depend on the selected sample size and they might exchange their importance in terms of their fractional variance when longer time series or different time periods are examined (Liu et al. 2008). However, both of them pass the prominent test of Monte-Carlo at the 95 % confidence level. Thus, the first three modes will be examined.

Figure 1 shows the spatial patterns of the first three MV-EOF modes and their corresponding time coefficients. As shown in Fig. 1a, MV-EOF1 displays a remarkable meridional tripole pattern, seen at the lower and upper level. At 850 hPa, it features an anticyclonic anomaly over the SCS–WNP and the Okhotsk Sea, respectively, and a cyclonic anomaly over the Meiyu-Baiu-Changma frontal area. This wave train pattern exhibits a baroclinic structure over the tropics and a barotropic structure to the north of  $30^\circ\text{N}$ . The prevailing period of PC1 is 2–3 years according to a continuous power spectrum analysis. The first mode is a mode with variations predominant on inter-annual time scale.

Apparently, the second mode expresses a distinct spatio-temporal character (Fig. 1b). It shows an equivalent barotropic anticyclonic anomaly over northern East Asia and associated weakened EASWJ. Over low latitudes, an anticyclonic circulation anomaly at 850 hPa which strengthen the lower-level southerly flow over the SCS, and anomalous northerly at 200 hPa are observed. These hint a meridional vertical overturning circulation, with anomalous descending motion over southern region of the SCS and ascending motion over South China. The time series of the second principal component presents remarkable inter-decadal variability with a period of 20–30 years but without a trend, indicating that MV-EOF2 represents the dominating mode of natural inter-decadal variability of the EASM. Two decadal changing points are identified in 1979 and 1993, respectively. This mode may capture the common features between the late 1970s change and the early 1990s change, which will be discussed later.

The spatial pattern of the third mode is characterized by enhanced northerly winds at the lower level over East China, enhanced southerly winds and weakened EASWJ at the upper level. The time series of PC3 displays an increasing trend accompanied by inter-annual variability. It indicates that the summer atmospheric circulation exhibits a

**Fig. 1** The (a) first, (b) second and (c) third MV-EOF modes of the EASM, showing the spatial patterns of (top) 850-hPa winds ( $\text{m s}^{-1}$ ), (middle) 200-hPa winds ( $\text{m s}^{-1}$ ) and (bottom) the corresponding time coefficients from 1958 to 2012. The red curve in c denotes the linear trend in PC3



**Fig. 2** Linear trends in East Asian summer a 850-hPa and b 200-hPa winds ( $\text{m s}^{-1} \text{ year}^{-1}$ ) derived from the ensemble average of JRA-55 and ERA-40 reanalysis data from 1958–2002

noteworthy weakening trend from 1958 to 2012. The spatial patterns of linear trends in summer 850 and 200-hPa winds are tested, as illustrated in Fig. 2. They are akin to the MV-EOF3 spatial pattern, especially for the features over low-latitude regions. This confirms that MV-EOF3 depicts the weakening trend in the EASM. This trend could be a signature of global warming as discussed by Xu et al. (2006). The PC3 levels off since the late 1990s, which is

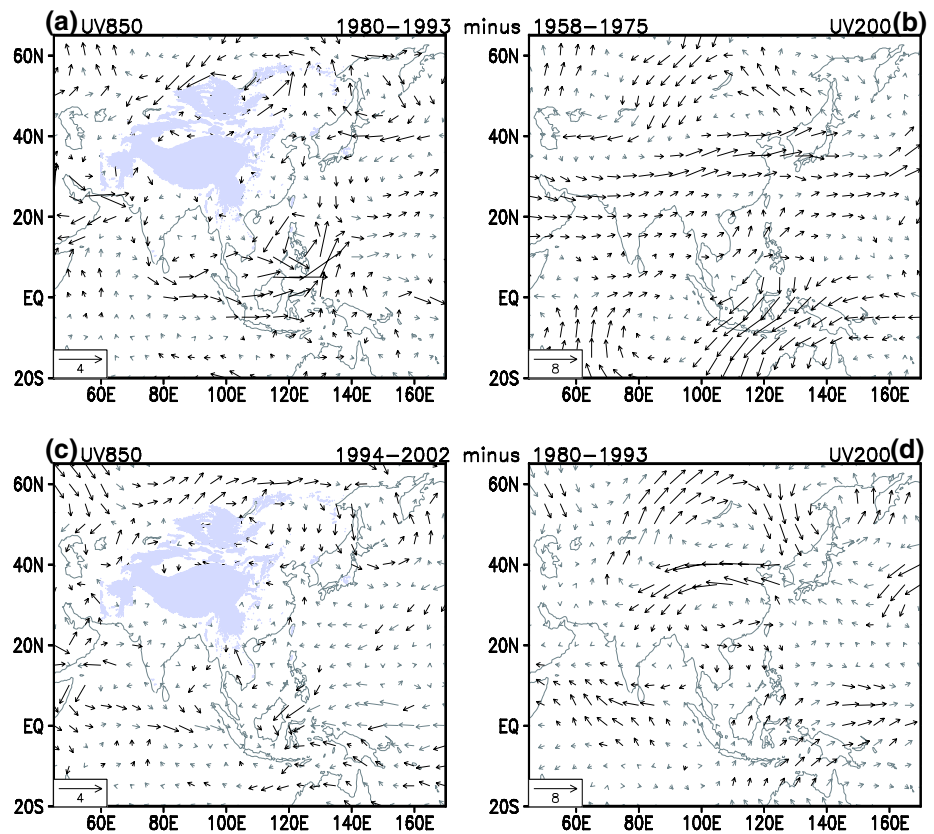
consistent with weak changes in global mean temperature during the same period (Solomon et al. 2010). One may notice that spatial patterns of the second and third modes are similar to some extent, even manifesting antisymmetric structures over the SCS-Philippines. It implies that there may be some nonnegligible interplay between natural decadal variability and anthropogenic climate change.

#### 4 Inter-decadal changes in the EASM

It has been revealed that the EASM experiences two distinct inter-decadal changes in the late 1970s and early 1990s, respectively. As indicated by analyses in the above section, so does the second mode of the EASM which is governed by natural decadal variability. It means that both these inter-decadal changes may be dominated by natural decadal variability. Figure 3 illustrates difference maps calculated from 1980–1993 mean minus 1958–1975 mean (Fig. 3a, b) and 1994–2002 mean minus 1980–1993 mean (Fig. 3c, d) for summer circulations.

For the first change around the end of 1970s, a barotropic cyclonic circulation anomaly over northern East Asia is observed, accompanied by an enhancement in EASWJ

**Fig. 3** Difference of the 1980–1993 mean minus 1958–1975 mean for summer, **a** 850-hPa and **b** 200-hPa winds ( $\text{m s}^{-1}$ ). **c, d** Differences of the 1994–2002 mean minus 1980–1993 mean. The *dark* wind vectors denote the 90 % confidence level by Student's *t* test



at 200 hPa. Over tropical regions, a prominent anomalous cyclone at the lower level appears near the Philippines, with strengthened northerly winds prevailing over the SCS and strengthened southerly anomalies over eastern Philippines (Fig. 3a), while an increase in divergence at upper level is detected around  $5^{\circ}\text{N}$ , accompanied by enhanced southerly winds over the SCS and northerly cross-equatorial flows (Fig. 3b). For the second change around the beginning of 1990s, on the whole, the feature is similar except for a switch in the sign of anomalies. A barotropic anticyclonic anomaly over north China and a lower-level anticyclone, enhanced upper-level convergence over the SCS-Philippines are seen (Fig. 3c, d). By comparison, both the spatial structures of circumfluent changes over the East Asian domain since the end of 1970s and since 1993 are similar to the pattern of MV-EOF2 shown in Fig. 1b. MV-EOF2 captures the common features between these inter-decadal changes in the EASM.

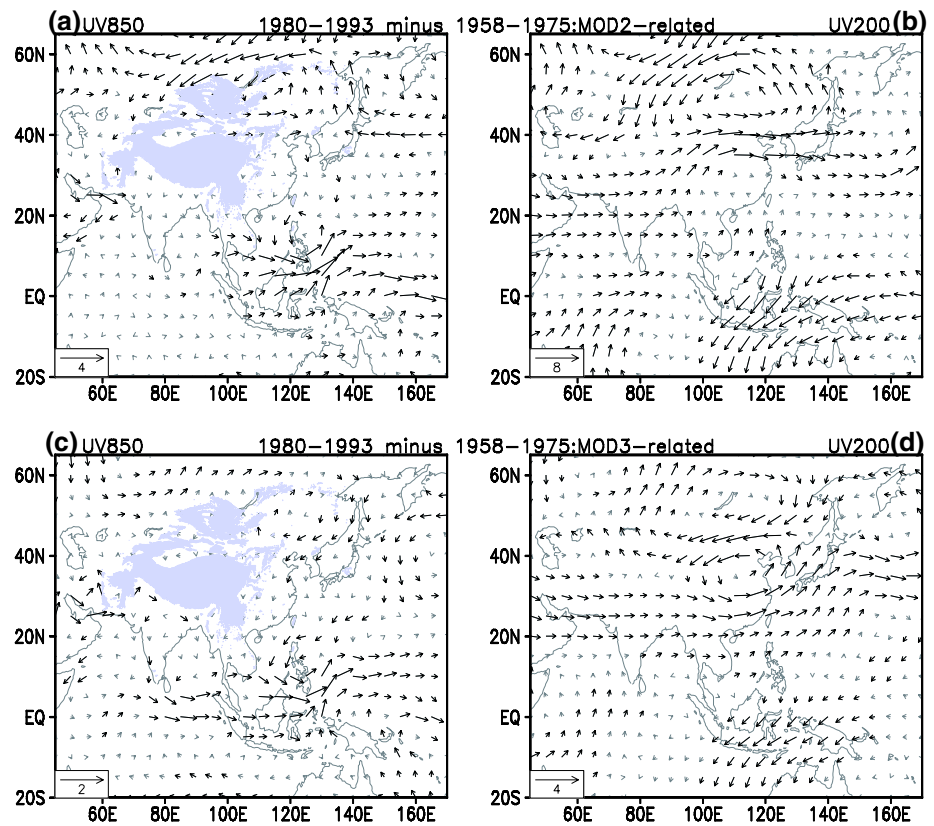
Moreover, antisymmetric structures are widespread rather than confined to East China. For the former change, over Eurasia, a zonal wave train of a barotropic structure controls the mid-latitudes to high latitudes north of  $40^{\circ}\text{N}$ , extending from the Ural Mountains to the Okhotsk Sea (Fig. 3a, b). A similar wave train with opposite anomalies is observed for the early 1990s change (Fig. 3c, d). Large-scale antisymmetric features indicate that there may be

some external forcing factors that may play roles in both of these inter-decadal changes.

What cannot be ignored is that some distinct characteristics exist, especially over the tropics. The circumfluent anomalies are more robust for the first change than for the second one. These inter-decadal changes may be dominated by natural decadal variability of the EASM, as discussed before. Different features imply that they may be modulated by anthropogenic factors, such as global warming. Could the EASM weakening trend related to global warming modify inter-decadal changes in the entire EASM system? What are the relative contributions of this trend and natural decadal variability?

Figure 4 shows changes in monsoon circulation from 1958–1975 to 1980–1993 for MVEOF2-related components (Fig. 4a, b) and MVEOF3-related components (Fig. 4c, d). MVEOF2-related and MVEOF3-related components are anomalies that linearly regressed onto PC2 and PC3, respectively. Apparently, spatial patterns of changes caused by natural decadal variability (Fig. 4a, b) are akin to those in Fig. 3a, b, and their magnitudes are equivalent, confirming that the second mode is most important in determining features of the first change. The EASM weakening trend reflected by the third mode results in an anomalous cyclone at 850 hPa over the Philippines and an increase in 200-hPa divergence since the 1980s (Fig. 4c, d). Changes related to

**Fig. 4** Difference of the 1980–1993 mean minus 1958–1975 mean for summer **a, c** 850-hPa and **b, d** 200-hPa winds ( $\text{m s}^{-1}$ ). Results in **a, b** are based on MVEOF2-related components, while in **c, d** are based on MVEOF3-related components. The dark vectors in **a–d** denote regions where wind speed anomalies are larger than 0.5, 1, 0.25 and 0.5  $\text{m s}^{-1}$ , respectively



MV-EOF3 are somewhat inconspicuous, with about half magnitudes of those variables related to MV-EOF2 over tropical East Asia. However, signals of natural decadal variability and global warming are overlying. Both of them make a positive contribution to the tropical circulation change occurring in the late 1970s. Situations for the early 1990s change are shown in Fig. 5. Similarly, natural decadal variability of the EASM makes the most important contribution. What differs from the former change is that parts of anomalies over the SCS-Philippines caused by MV-EOF2 are offset by anomalies caused by MV-EOF3. Consequently, the total anomalies are weaker in contrast to the 1970s change (Fig. 3). This amplitude asymmetry may be partly attributed to different contributions of the weakening trend associated with global warming. The contributions of MV-EOF1 mode to these two changes are negligible, accounting for only about one-eighth of total changes (figure not shown).

Monsoon circulations are coupled with monsoon precipitation. Here, we illustrate relative contributions of natural decadal variability of monsoon system and its weakening trend to climate changes occurring around the end of 1970s and beginning of 1990s. For the change from 1958–1975 to 1980–1993, summer total precipitation anomaly features an increase in rainfall over central East China and Northeast China, but a decrease in rainfall over North China and South China (Fig. 6a), which is consistent with Ding et al.

(2008). As shown in Fig. 6b, precipitation anomaly caused by natural decadal variability displays a meridional quadrupole structure, which is consistent with circumfluent anomaly in Fig. 4a, b. The anomalous cyclone over northern East China is accompanied by an increase in lower-tropospheric convergence and mid-tropospheric ascent (not shown), leading to increased precipitation. An enhancement in the EASWJ at 200 hPa (Fig. 4b) may increase precipitation over the Yangtze River Valley, but decrease precipitation over North China (Shi and Zhang 2008). Precipitation over South China reduces as a result of the meridional vertical overturning circulation. The late 1970s climate change mainly arises from natural decadal variability of the EASM system. In South China and Northeast China, its contributions can be up to 80 %, while in North China and central East China, the contributions are about 50 and 30 %, respectively (Fig. 6d). On the other hand, the weakening trend in the EASM brings more precipitation to areas south of 33°N and less precipitation to northern China (Fig. 6c) because of reduced southerly water vapor transport to North China (not shown). The dipole rainfall pattern resembles the linear trend in summer total precipitation (Lei et al. 2011). Contribution of the weakening trend to the first inter-decadal change is relatively small, but it can contribute 40–50 % to precipitation change over North China and central East China (Fig. 6e).

**Fig. 5** As in Fig. 4, but for the difference of the 1994–2002 mean minus 1980–1993 mean

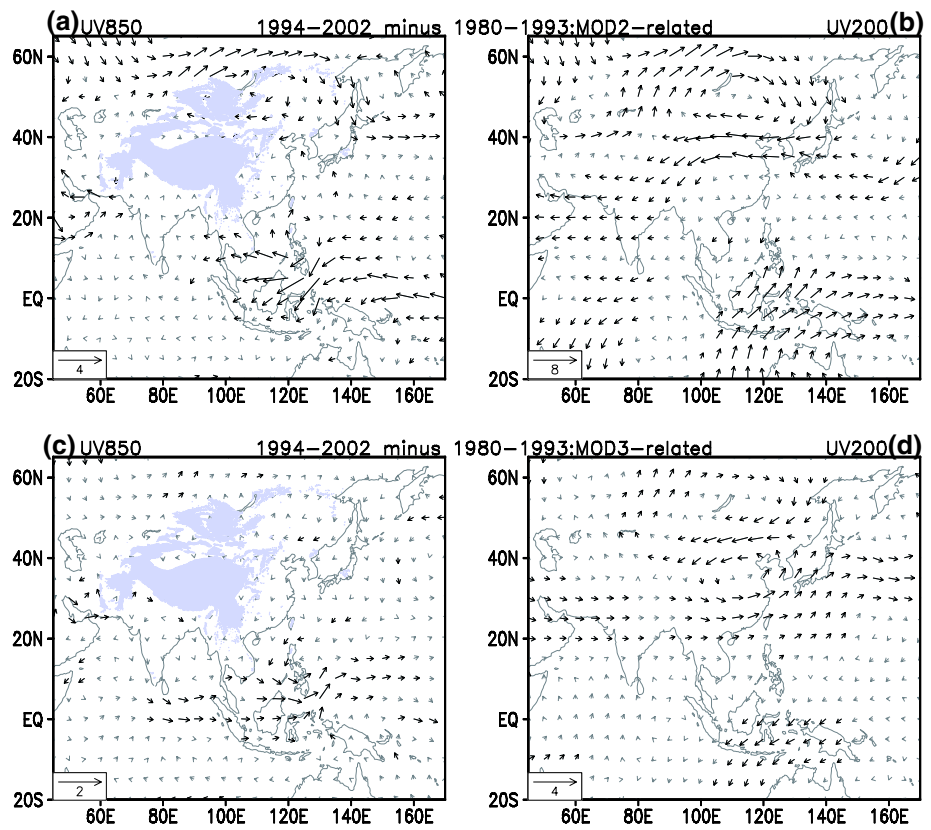
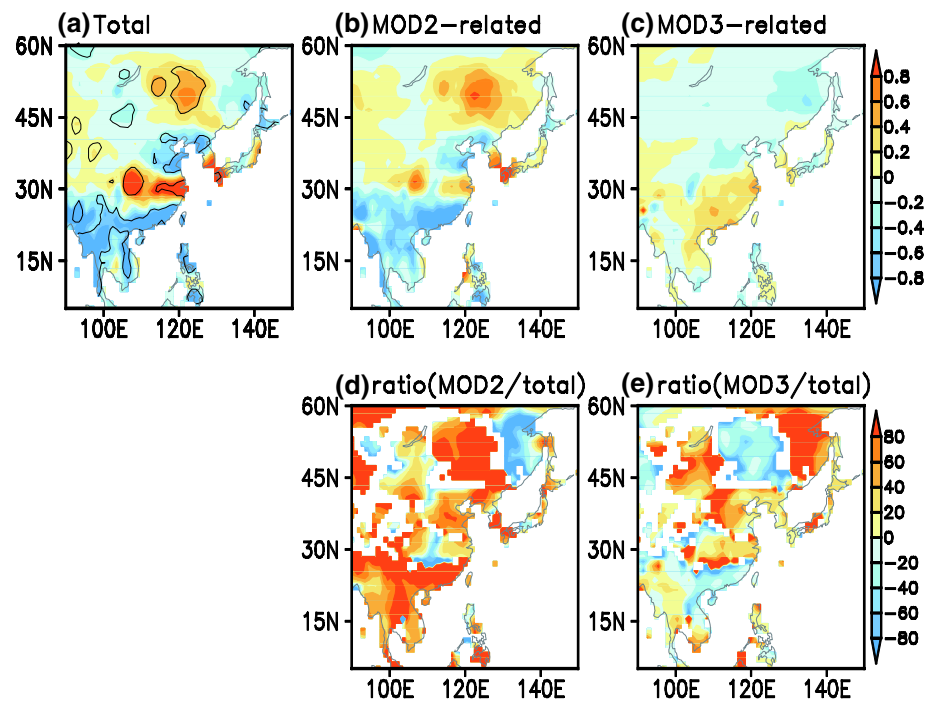


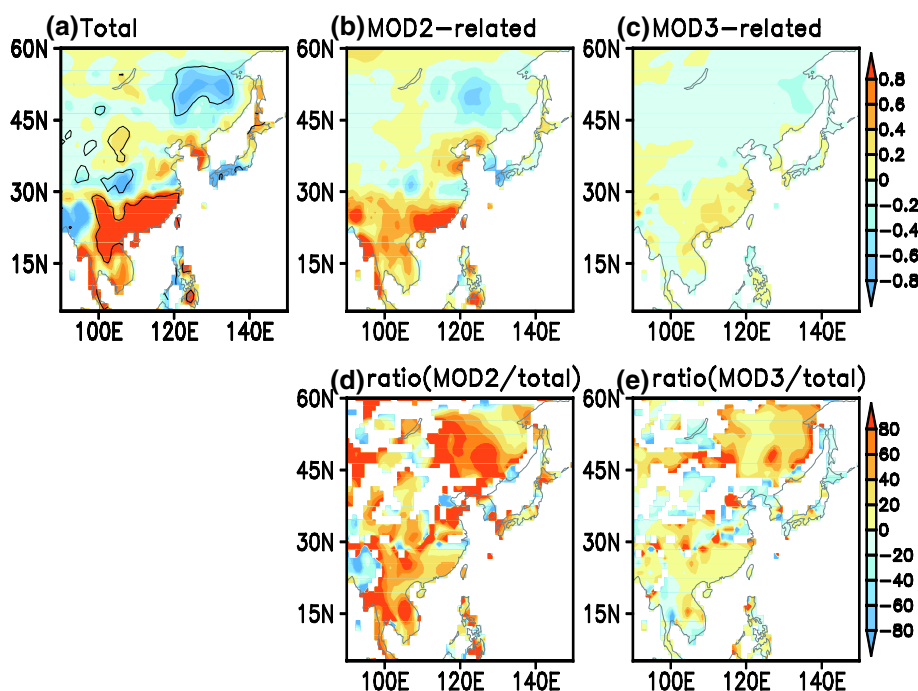
**Fig. 6** Difference of the 1980–1993 mean minus 1958–1975 mean for summer precipitation ( $\text{mm day}^{-1}$ ) based on **a** total field, **b** MVEOF2-related component and **c** MVEOF3-related component. Percent (%) of precipitation change due to **d** MV-EOF2 and **e** MV-EOF3. The black contours in **a** denote regions where the difference is significant at the 90 % confidence level according to the Student's *t* test



Similarly, precipitation change around 1993 is mainly associated with the MV-EOF2, and modified by the MV-EOF3 (Fig. 7). Consistent with monsoon circulation, parts

of inter-decadal change of precipitation after 1993 caused by decadal variability are offset by those related to global warming. That may explain partly why climate change

**Fig. 7** As in Fig. 6, but for the difference of the 1994–2002 mean minus 1980–1993 mean



signals are indistinctive over North China and central China (Fig. 7a). It is noteworthy that contribution of natural decadal variability drops to about 40 % in South China (Fig. 7d). For the climate change in the early 1990s, situation is quite complicated. The intraseasonal oscillation and synoptic-scale disturbance may have an influence (Kwon et al. 2007; Chen et al. 2012, 2015).

## 5 Associations with remote SST anomaly in the SIO

The analyses in the above section indicate that inter-decadal variation of the EASM for the period 1958–2012 is governed by natural decadal variability, and further modified by a weakening trend. And the relative linear contributions of this trend to the late 1970s change and the early 1990s change are totally different. In order to find some common SST forcing, we focus on natural decadal variability of ocean–atmosphere system. Thus, in the analysis hereinafter, all linear trends in raw data are removed if there is no extra instruction.

Inter-decadal variability of the EASM is closely correlated with the IPO, as seen from Fig. 8a. Around the late 1970s, the IPO transits from a cold phase to a warm phase (Wang et al. 2012), manifesting an El-Niño like decadal warming (Fig. 8c). It has been revealed that associated tropical Pacific SST anomaly is one of the key factors causing a weakening in the Asian summer monsoon (Chang et al. 2000; Ding et al. 2008, 2009). SST in the Pacific Ocean undergoes a weak La-Niña like decadal cooling

from 1980–1993 to 1994–2002 (Fig. 8d). However, in contrast to the former change, SST anomaly in the equatorial eastern Pacific seems insignificant. That is because another phase transition of the IPO since the 1980s occurs in the end of the 1990s rather than around the 1993/4 (Wang et al. 2012). Inter-decadal changes in the EASM and the IPO are asynchronous in the 1990s. The WNP SST anomalies may result from atmospheric changes as discussed by Wu et al. (2010), rather than be one of factors contributing to the monsoon change. Some study indicates the La-Niña like decadal cooling may exert impacts on the monsoon and climate change in the early 1990s (Yuan and Chen 2013; Zhu et al. 2014). Nevertheless, linear contribution of the IPO to the second change in the EASM may be relatively small.

On the other hand, the EASM is negatively correlated with SST anomalies in the IO basin (Fig. 8a). Han et al. (2014) showed that a basin-wide warming/cooling pattern dominates IO SST anomalies on the decadal time scale. The basin-wide pattern displays a decadal warming trend since the late 1970s, but displays a cooling trend after 1993. Decadal trends are more significant in the SIO than that in the equatorial and northern IO where SST shows a distinct linear trend (Fig. 8c, d). Further studies find that phase transitions of SST anomaly in the SIO are synchronous with natural decadal changes in the EASM (Fig. 8b). Moreover, a decadal warming is accompanied by an increase in mid-tropospheric ascent, and vice versa (not shown). The correlation between SST anomalies and 500-hPa vertical p velocity over SIO is  $-0.71$ , which is significant at the 99 % confidence level. That is, on decadal time scale, the SST could be a factor for the atmospheric circulation change



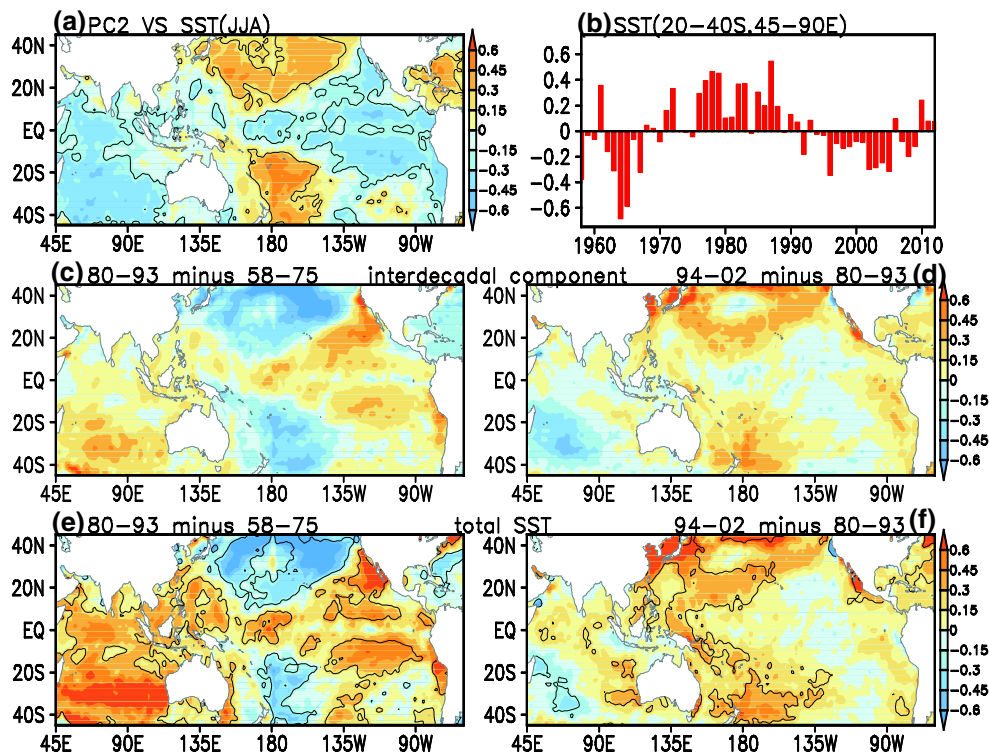


**Fig. 8** **a** Correlations of summer SST with PC2. **b** Time series of the anomalous summer SST ( $^{\circ}\text{C}$ ) averaged over SIO ( $20^{\circ}\text{--}40^{\circ}\text{S}$ ,  $45^{\circ}\text{--}90^{\circ}\text{E}$ ). Difference of the 1980–1993 mean minus 1958–1975 mean for summer SST ( $^{\circ}\text{C}$ ) for **c** inter-decadal component and **e** total field.

**d**, **f** Differences of the 1994–2002 mean minus 1980–1993 mean. The *black contours* in **a**, **e** and **f** denote regions where the correlation or difference is significant at the 90 % confidence level

over East Asia. What's more, change of total SST in the SIO from 1980–1993 to 1994–2002 features a significant cooling, which is opposite to change from 1958–1975 to 1980–1993 even under the background of notable global warming (Fig. 8e, f). Remote SIO SST anomaly may be responsible for both inter-decadal changes of the EASM that occurred around 1979 and 1993.

Figure 9 shows the regressed maps with respect to inter-decadal component of regional mean SST averaged over  $45^{\circ}\text{--}90^{\circ}\text{E}$ ,  $20^{\circ}\text{--}40^{\circ}\text{S}$ . The following descriptions correspond to a cold SST anomaly phase, but also apply to a warm SST anomaly phase except for a switch in the sign of anomalies. As expected, a large-scale IO cooling pattern is observed with a large center over the western SIO (Fig. 9a). A decadal cooling is accompanied by an anomalous mid-tropospheric descent, lower-level divergence, and upper-level convergence west of  $90^{\circ}\text{E}$  (Fig. 9b–f). Notable mid-tropospheric ascents are found from the eastern SIO to western Australia and over the tropical IO, respectively (Fig. 9b). The anomalous vertical movements concur with remarkable increase in convergence at 850 hPa and divergence at 200 hPa (Fig. 9c–f). The divergent winds are more remarkable over the tropical regions than over the subtropics. Atmospheric anomalies could not be explained by

local SST anomalies as negative SST anomalies are seen in the eastern SIO and tropical IO (Fig. 9a). Instead, they may be induced by cooling in the western SIO through changes of the east–west temperature gradient in the subtropical regions and south–north SST gradient between the SIO and equatorial IO (Lindzen and Nigam 1987). At the upper level, outflows from the eastern SIO and tropical IO converge over the Philippines, leading to regional enhanced descent and anomalous lower-level divergence (Fig. 9b–d). An anomalous anticyclone is observed at 850 hPa over the SCS-Philippines in Fig. 9e and pronounced cross-equatorial flows are present from the subtropics of the Southern Hemisphere at 200 hPa in Fig. 9f, which is akin to spatial patterns associated with MV-EOF2 (Figs. 1b, 4a, b, 5a, b). Above analyses confirm that SST forcing in subtropical IO could exert an effect on monsoon circulation over tropical East Asia through anomalous vertical circulation. Besides, a barotropic zonal wave train is observed along  $50^{\circ}\text{N}$  over the Eurasian region (Fig. 9e, f), similar to those in Figs. 3, 4 and 5. But the possible connection from the western SIO SST to the mid-high latitudinal circulation is still unknown.

Figure 10 shows difference maps for summer lower-level winds, mid-level p-vertical velocity, upper-level winds and divergence based on inter-decadal components

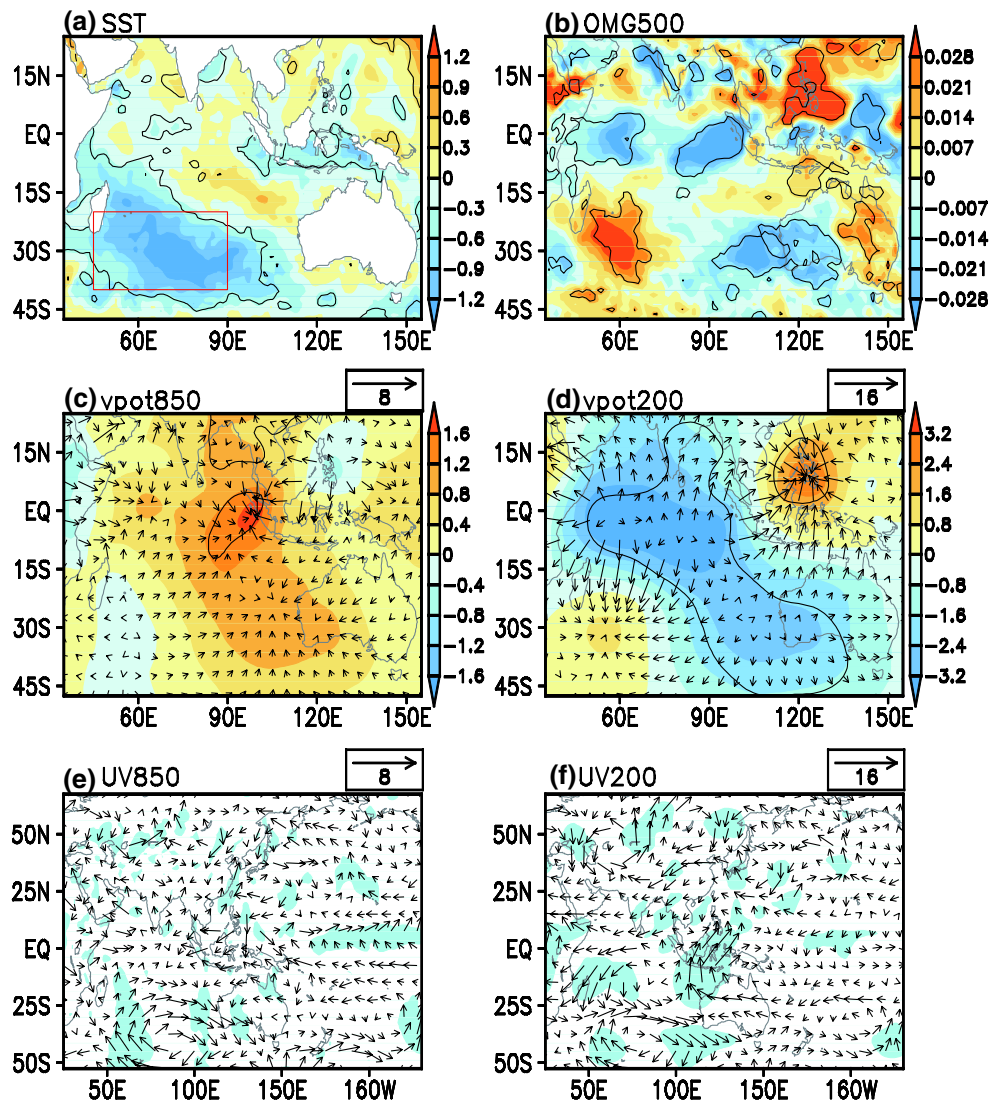


**Fig. 9** The regressed summer **a** SST ( $^{\circ}\text{C}$ ), **b** 500-hPa vertical p velocity ( $\text{Pa s}^{-1}$ ), **c** 850-hPa velocity potential and divergent winds ( $10^6 \text{ m}^2 \text{ s}^{-1}$ ), **d** 200-hPa velocity potential and divergent winds ( $10^6 \text{ m}^2 \text{ s}^{-1}$ ), **e** 850-hPa and **f** 200-hPa winds ( $\text{m s}^{-1}$ ) anomalies with

respect to inter-decadal component of regional mean SST over SIO [boxed area in **a**]. The black contours in **a–d** and the shadings in **e, f** denote regions where the correlation is significant at the 90 % confidence level

for the late 1970s change and early 1990s change, respectively. Since the 1980s, the SIO SST decadal warming shown in Fig. 8c concurs with an anomalous cyclone at 850 hPa, an increase in ascent at 500 hPa and a divergence at 200 hPa over the SCS-Philippines. An increase in upper-level convergence along with anomalous mid-tropospheric descent over the western Australia and equatorial IO are also seen (Fig. 10a, b). The northerly cross-equatorial flows from tropical East Asia to subtropical SIO in the upper troposphere are quite clear. Situations for the change from pre-1993 to post-1993 are nearly opposite (Fig. 10c, d). The composited results indicate a linkage between the remote SIO SST and EASM discussed in above for both these inter-decadal changes.

To further demonstrate possible influence of remote SIO SST forcing on the EASM, two simple numerical experiments with the CAM4.0 described in Sect. 2 are carried out: one with climatological seasonal cycle of SST and the other with climatological seasonal cycle of SST plus idealized JJA SST anomalies of  $-0.3 \text{ }^{\circ}\text{C}$  in the region of  $45^{\circ}\text{--}90^{\circ}\text{E}$  and  $20^{\circ}\text{--}40^{\circ}\text{S}$  (Fig. 11a). The model is integrated for 20 years and only the last 10 years simulation results are used in the analysis. Chen et al. (2014) showed that the CAM4 control run can well capture the spatial feature of the summer climatology over the tropics and extra-tropics ( $60^{\circ}\text{S}\text{--}60^{\circ}\text{N}$ ) in observations. On this basis, the difference of atmospheric response between experiments SIO\_SST and CAM4\_Control is shown in Fig. 11. In response to

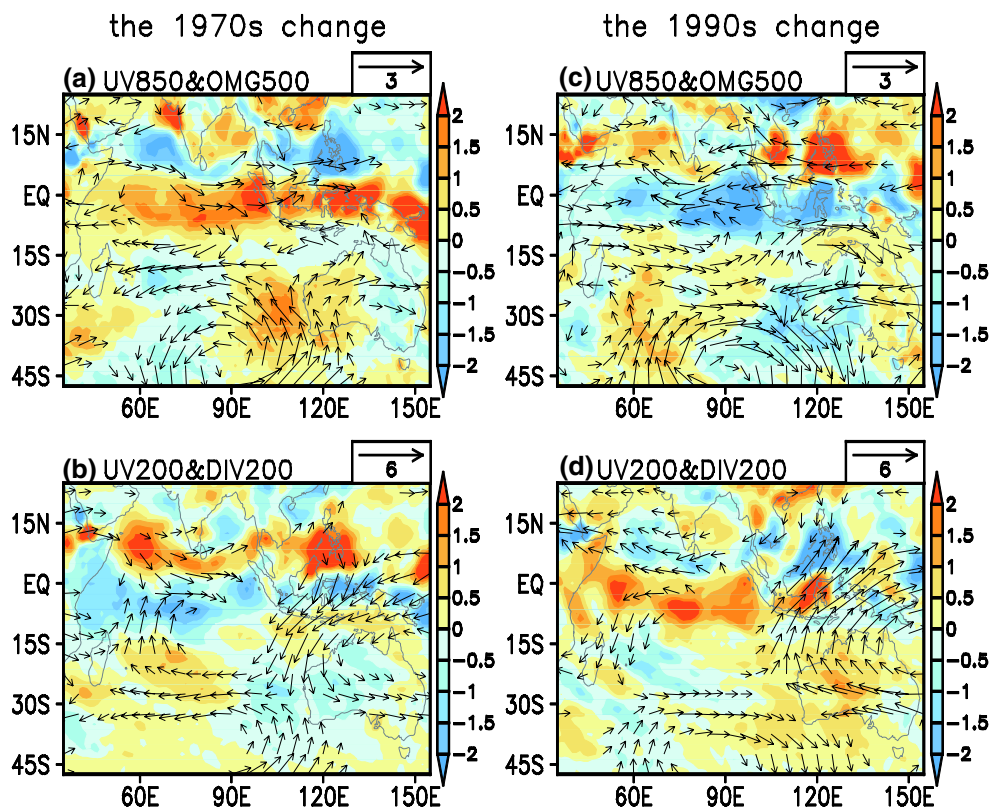


**Fig. 10** Difference of the 1980–1993 mean minus 1958–1975 mean for summer **a** 850-hPa winds (vector,  $\text{m s}^{-1}$ ) and 500-hPa p-vertical velocity (shading,  $0.01 \text{ Pa s}^{-1}$ ), **b** 200-hPa winds (vector,  $\text{m s}^{-1}$ ) and divergence (shading,  $10^{-6} \text{ s}^{-1}$ ) for inter-decadal components. **c**, **d**

Differences of the 1994–2002 mean minus 1980–1993 mean. At the lower level, vectors are plotted only where their wind speed anomalies are larger than  $0.5 \text{ m s}^{-1}$ , while the threshold value is  $1 \text{ m s}^{-1}$  at the upper level

the SIO cooling (Fig. 11a), the regional descent tends to intensify, while the developments of ascent are seen over the western Australia and tropical IO (Fig. 11c), which are accompanied by outflows to the Philippines at the upper level (Fig. 11d, e). The consequent increase in convergence at 200 hPa over the tropical WNP is accompanied by an anomalous mid-tropospheric descent and lower-tropospheric divergence (Fig. 11b, c). In particular, an anomalous anticyclone at 850 hPa appears over the SCS-Philippines (Fig. 11c), which bears similarity to the observational composite in Fig. 10c. However, the location of anomalies over the SIO displays some differences from observations. Albeit this discrepancy, the model results support the impact of remote SIO SST forcing on the tropical East Asian circulation.

## 6 Summary and discussion

On the basis of JRA-55 Reanalysis dataset for the period 1958–2012, a study of variability on longer time scales of the entire EASM system has been undertaken. A MV-EOF analysis shows that the dominating pattern of

natural decadal variability of monsoon circulation features an equivalent barotropic anticyclonic circulation anomaly over northern East Asia and a meridional vertical overturning circulation over the tropics, which is represented by the second mode of variability of the EASM. Its corresponding time coefficient exhibits two remarkable changing points that occur in 1979 and 1993, with a period of 20–30 years. Besides, as indicated by the third mode, a persistent weakening trend in the EASM has been confirmed, which could be a signature of global warming.

The present study focuses on substantial inter-decadal changes in the EASM that occur around the late 1970s and early 1990s, respectively. The observational results indicate that characteristics of these two changes share some common features due to natural decadal variability. For the first change in the end of 1970s, it features a zonal wave train of a barotropic structure extending from the Ural Mountains to the Okhotsk Sea, an anomalous lower-level cyclone near the Philippines, and an increase in upper-level divergence around  $5^\circ\text{N}$ . For the second change in the early 1990s, on the whole, the spatial structure is similar except for a switch in the sign of anomalies. Opposite circulation anomalies over mid-high latitudes are more significant. On

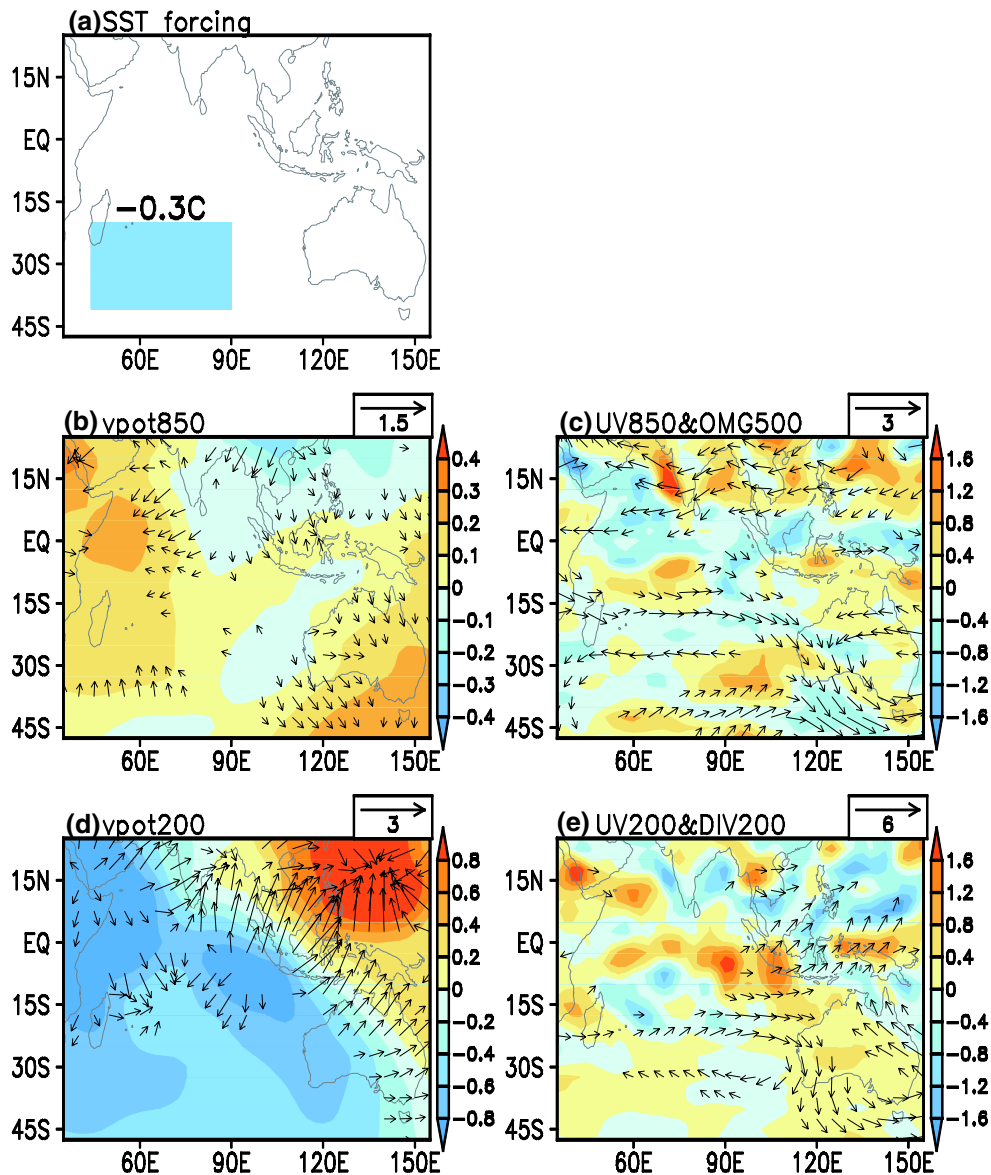


**Fig. 11** a The SST anomalies specified in the sensitive experiment, composite differences of **b** 850-hPa velocity potential and divergent winds ( $10^6 \text{ m}^2 \text{ s}^{-1}$ ), **c** 850-hPa winds (vector,  $\text{m s}^{-1}$ ) and 500-hPa p-vertical velocity (shading,  $0.01 \text{ Pa s}^{-1}$ ), **d** 200-hPa velocity potential and divergent winds ( $10^6 \text{ m}^2 \text{ s}^{-1}$ ), **e** 200-hPa winds (vector,

$\text{m s}^{-1}$ ) and divergence (shading,  $10^{-6} \text{ s}^{-1}$ ) in JJA between experiments of negative SIO SST and CAM4 control. Divergent winds in **b** and **d** are plotted only where their anomalies are larger than 0.25 and  $0.5 \text{ m s}^{-1}$ , respectively. Vectors in **c** and **e** are plotted only where their wind speed anomalies are larger than 0.5 and  $1 \text{ m s}^{-1}$ , respectively

the other hand, some distinct characteristics are observed. In contrast to the 1970s change, tropical atmospheric circulation change signals from 1980–1993 to 1994–2002 are relatively infirm. This amplitude asymmetry is partly attributed to different contributions of the weakening trend in the EASM to these two inter-decadal changes. To summarize, these changes are mainly regulated by natural decadal variability, while further modified by a persistent weakening trend in monsoon system.

The EASM circulation is coupled with precipitation over East China. Coherently, for two summer climate

changes in the end of 1970s and beginning of 1990s, natural decadal variability of monsoon is most important in determining corresponding change patterns. This conclusion is consistent with Lei et al. (2011), who explored the interplay between natural decadal variability and anthropogenic climate change in summer rainfall over China. In comparison, the climate change around 1993 featuring an increase in precipitation over South China is more complicated. Not only variability on longer time scales but also the intraseasonal oscillation and

synoptic-scale disturbance may play roles (Kwon et al. 2007; Chen et al. 2012, 2015).

Common characteristics between these inter-decadal changes implicates that some external forcings may be responsible for both of them. Here we concern plausible influence of SST anomaly in the SIO, mainly because phase transitions of the SST anomaly are synchronous with natural decadal changes in the EASM and the SST could be an important factor influencing atmospheric circulation. Regression analysis results indicate that a decadal cooling in the SIO may induce an anomalous middle-level descent over the western SIO, while anomalous ascents extend from the eastern SIO to western Australia and over the tropical IO. The accompanying upper-level divergent flows from the eastern SIO and equatorial IO to tropical East Asia lead to anomalous descent and an anomalous lower-level anticyclone over the SCS-Philippines. The linkage between the SIO SST forcing and EASM can apply to both of the late 1970s change and the early 1990s change, according to a composite analysis. Moreover, this linkage

can be basically reproduced by numerical experiments with the CAM4. Wu et al. (2010) discussed an increase SST in the equatorial IO since the early 1990s that could enhance regional lower-level convergence and ascent, further leading to the development of a lower-level anticyclone over the SCS-subtropical WNP through anomalous vertical circulation. Both observations and simulations show that the SIO decadal cooling after 1993 may also promote observed tropical atmospheric circulation anomalies.

Previous studies have investigated the linkage between subtropical SIO SST anomalies and the EASM variability. Especially, the Indian Ocean Subtropical Dipole (Behera and Yamagata 2001), which is a leading mode of inter-annual variability of SST, is thought to be one of important factors that can affect East Asian circulation and precipitation (Suzuki et al. 2004; Yang and Ding 2007; Cao et al. 2014). However, little is known about its impact on the inter-decadal time scales. Xue (2001) proposed that the subtropical SIO SST anomaly plays a key role in the long-term variation of EASM, but with the detailed processes

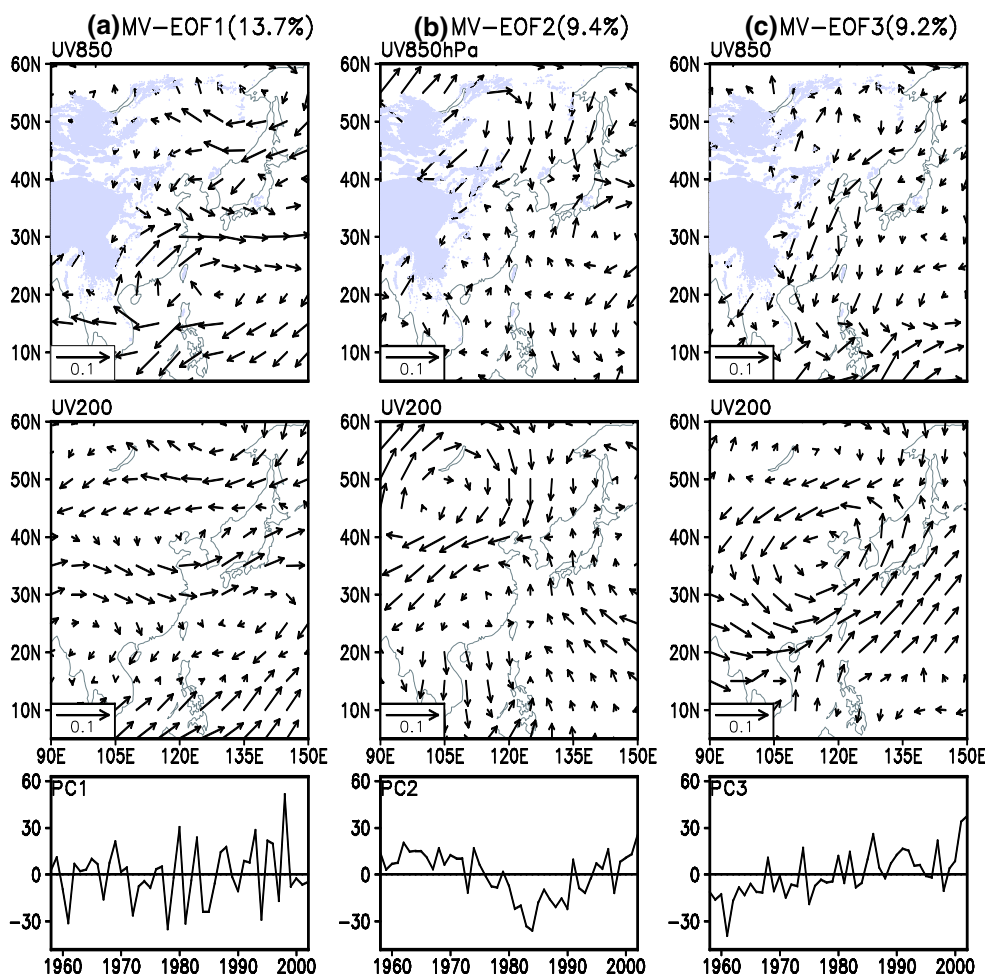


Fig. 12 The same as in Fig. 1 except based on ERA-40 data from 1958–2002

remaining to be unravelled. The present study suggests possible contributions of the SIO SST anomalies to inter-decadal changes in the East Asian monsoon, which may help improve the understanding of physical mechanism involved with the EASM variability.

It is necessary to discuss the validness of results based on JRA-55 data on the inter-decadal variations. We performed a parallel analysis using the ERA-40 Reanalysis dataset that is available for the period 1958–2002 which contains the main periods we focus on. By comparison, results derived from these two datasets are relatively consistent. Due to the limited space, only the MV-EOF analysis results are presented in Fig. 12. One can find that patterns of the first three leading modes based on ERA-40 data are extremely similar to those based on JRA-55 data shown in Fig. 1, except the anticyclone at 850 hPa over the Philippines related to MV-EOF2 is somewhat infirm. Besides, the time series of these principal components express pronounced inter-annual variation, natural decadal variation and a persistent linear trend, respectively. PC2 also reflects two changing points of natural decadal variability: one in the end of 1970s and the other in the beginning of 1990s. Overall, both the JRA-55 and ERA-40 data depict common characteristics between the late 1970s change and the early 1990s change, and their amplitude asymmetry over the tropics. In addition, we examined the precipitation changes based on monthly rainfall data at 160 stations in China. The obtained results (figures not shown) confirm the precipitation change patterns and relative contributions of the MV-EOF2 and MV-EOF3.

**Acknowledgments** The authors thank the editor and two reviewers for their comments and suggestions which led to an improved manuscript. This research was jointly supported by National Natural Science Foundation of China (41530503, 41175076), National Key Basic Research and Development Projects of China (2014CB953901). RW acknowledges the support of National Natural Science Foundation of China grants (41275081 and 41475081). HZ acknowledges the support of the high-performance grid computing platform of Sun Yat-sen University.

## References

- Behera SK, Yamagata T (2001) Subtropical SST dipole events in the Southern Indian Ocean. *Geophys Res Lett* 28:327–330
- Cao J et al (2014) Summer rainfall variability in low-latitude highlands of China and subtropical Indian ocean dipole. *J Clim* 27:880–892
- Chang CP, Zhang YS, Li T (2000) Interannual and interdecadal variations of the East Asian summer monsoon and tropical Pacific SSTs. Part I: roles of the subtropical ridge. *J Clim* 13:4310–4325
- Chen WY (1982) Fluctuation in Northern Hemisphere 700 mb height field associated with the Southern Oscillation. *Mon Wea Rev* 110:802–823
- Chen LX, Xie A (1988) Westward propagating low-frequency oscillation and its teleconnection in the eastern hemisphere. *Acta Meteorologica Sinica* 2:300–312
- Chen LX, Yang JH, Wang G (1989) Evolutional features of interannual low-frequency oscillations and their relation to the occurrence of El Niño. *Acta Meteorologica Sinica* 3:352–365
- Chen LX, Chen D, Shen RG (1990) The interannual oscillation of rainfall over China and its relation to the interannual oscillation of the air-sea system. *Acta Meteorologica Sinica* 4:598–612
- Chen JP, Wu R, Wen ZP (2012) Contribution of South China sea tropical cyclones to an increase in Southern China summer rainfall around 1993. *Adv Atmos Sci* 29:585–598
- Chen ZS et al (2014) Influence of two types of El Niños on the East Asian climate during boreal summer: a numerical study. *Clim Dyn* 43:469–481. doi:10.1007/s00382-013-1943-1
- Chen JP et al (2015) Influences of northward propagating 25–90-day and quasi-biweekly oscillations on eastern China summer rainfall. *Clim Dyn* 45:105–124. doi:10.1007/s00382-014-2334-y
- Ding YH, Wang ZY, Sun Y (2008) Inter-decadal variation of the summer precipitation in East China and its association with decreasing Asian summer monsoon. Part I: observed evidences. *Int J Climatol* 28:1139–1161
- Ding YH et al (2009) Inter-decadal variation of the summer precipitation in East China and its association with decreasing Asian summer monsoon. Part II: possible causes. *Int J Climatol* 29:1926–1944
- Guan B, Johnny CLC (2006) Nonstationary of the intraseasonal oscillations associated with the Western North Pacific summer monsoon. *J Clim* 19:622–629
- Guo QY et al (2003) Interdecadal variability of East Asian summer monsoon and its impact on the climate of China. *Acta Geogr Sin* 58:569–576 (in Chinese)
- Han WQ et al (2014) Intensification of decadal and multi-decadal sea level variability in the western tropical Pacific during recent decades. *Clim Dyn* 43:1357–1379. doi:10.1007/s00382-013-1951-1
- Ju JH, Qian C, Cao J (2005) The intraseasonal oscillation of east Asian summer monsoon. *Chin J Atmos Sci* 29:187–194 (in Chinese)
- Kajikawa Y, Wang B (2012) Interdecadal change of the South China sea summer monsoon onset. *J Clim* 25:3207–3218
- Kobayashi S et al (2015) The JRA-55 reanalysis: general specifications and basic characteristics. *J Meteor Soc Jpn* 93:5–48
- Kwon MH et al (2005) Decadal change in relationship between east Asian and WNP summer monsoons. *Geophys Res Lett* 32:L16709. doi:10.1029/2005GL020326
- Kwon MH, Jhun JG, Ha KJ (2007) Decadal change in east Asian summer monsoon circulation in the mid-1990s. *Geophys Res Lett* 34:L21706. doi:10.1029/2007GL031977
- Lei YH, Hoskins B, Slingo J (2011) Exploring the interplay between natural decadal variability and anthropogenic climate change in summer rainfall over China. Part I: observational evidence. *J Clim* 24:4584–4599
- Li TM et al (2006) Spatiotemporal structures and mechanisms of the tropospheric biennial oscillation in the Indo Pacific warm ocean regions. *J Clim* 19:3070–3080
- Li HM et al (2010) Responses of East Asian summer monsoon to historical SST and atmospheric forcing during 1950–2000. *Clim Dyn* 34:501–514
- Lindzen RS, Nigam S (1987) On the role of sea surface temperature gradients in forcing low-level winds and convergence in the tropics. *J Atmos Sci* 44:2418–2436
- Liu J, Wang B, Yang J (2008) Forced and internal modes of variability of the East Asian summer monsoon. *Clim Past* 4:225–233
- Liu Y, Huang G, Huang RH (2011) Inter-decadal variability of summer rainfall in Eastern China detected by the Lepage test. *Theor Appl Climatol* 106:481–488
- Mao JY, Chan JC (2005) Intraseasonal variability of the South China Sea summer monsoon. *J Clim* 18:2388–2402

- Meehl A, Arblaster JM (2002) The tropospheric biennial oscillation and Asian-Australian monsoon rainfall. *J Clim* 15:722–744
- Neale RB et al (2013) The mean climate of the community atmosphere model (CAM4) in forced SST and fully coupled experiments. *J Clim* 26:5150–5168. doi:[10.1175/JCLI-D-12-00236.1](https://doi.org/10.1175/JCLI-D-12-00236.1)
- New M, Hulme M, Jones P (2000) Representing twentieth-century space–time climate variability. Part II: development of 1901–1996 monthly grids of terrestrial surface climate. *J Clim* 13:2217–2238
- Nitta T, Hu ZZ (1996) Summer climate variability in china and its association with 500 hPa height and tropical convection. *J Meteor Soc Jpn* 74:425–445
- Nitta T, Yamada S (1989) Recent warming of tropical sea surface temperature and its relationship to the northern hemisphere circulation. *J Meteor Soc Jpn* 67:375–383
- North GR et al (1982) Sampling errors in the estimation of empirical orthogonal functions. *Mon Wea Rev* 110:699–706
- Rayner NA et al (2003) Global analyses of sea surface temperature, sea ice, and night marine air temperature since the late nineteenth century. *J Geophys Res-Atmos* 108:D14. doi:[10.1029/2002JD002670](https://doi.org/10.1029/2002JD002670)
- Shi YY, Zhang YC (2008) The impacts of intensity variations of the East Asia Subtropical Westerly Jet on summer precipitation in North China. In: Proceedings of the 25th Chinese Meteorological Society annual meeting, pp 625–634
- Solomon S et al (2010) Contributions of stratospheric water vapor to decadal changes in the rate of global warming. *Science* 327:1219. doi:[10.1126/science.1182488](https://doi.org/10.1126/science.1182488)
- Suzuki R et al (2004) Indian Ocean subtropical dipole simulated using a coupled general circulation model. *J Geophys Res* 109:C09001. doi:[10.1029/2003JC001974](https://doi.org/10.1029/2003JC001974)
- Trenberth K, Hurrell J (1994) Decadal atmosphere-ocean variations in the Pacific. *Clim Dyn* 9:303–319. doi:[10.1007/BF00204745](https://doi.org/10.1007/BF00204745)
- Uppala SM et al (2005) The ERA-40 re-analysis. *QJR Meteor Soc* 131:2961–3012. doi:[10.1256/qj.04.176](https://doi.org/10.1256/qj.04.176)
- Wang B (1992) The vertical structure and development of the ENSO anomaly mode during 1979–1989. *J Atmos Sci* 49:698–712
- Wang HJ (2001) The weakening of the Asian monsoon circulation after the end of 1970s. *Adv Atmos Sci* 18:376–386
- Wang B et al (2012) Recent change of the global monsoon precipitation (1979–2008). *Clim Dyn* 39:1123–1135. doi:[10.1007/s00382-011-1266-z](https://doi.org/10.1007/s00382-011-1266-z)
- Wu R, Chen LT (1998) Decadal variation of summer rainfall in the Yangtze-Huaihe River reaches and its relationship to atmospheric circulation anomalies over East Asia and western North Pacific. *Adv Atmos Sci* 15:510–522
- Wu R, Kinter JL III, Kirtman BP (2005) Discrepancy of interdecadal changes in the Asian region among the NCEP-NCAR reanalysis, objective analyses, and observations. *J Clim* 18:3048–3067
- Wu BY et al (2008) Distinct modes of the east asian summer monsoon. *J Clim* 21:1122–1138
- Wu BY, Zhang RH, Wang B (2009) On the association between spring arctic sea ice concentration and chinese summer rainfall: a further study. *Adv Atmos Sci* 26:666–678
- Wu R et al (2010) An interdecadal change in southern china summer rainfall around 1992/93. *J Clim* 23:2389–2403
- Xiang BQ, Wang B (2013) Mechanisms for the advanced Asian summer monsoon onset since the mid-to-late 1990s. *J Clim* 26:1993–2009
- Xu M et al (2006) Steady decline of East Asian monsoon winds, 1969–2000: evidence from direct ground measurements of wind speed. *J Geophys Res* 111:D24111. doi:[10.1029/2006JD007337](https://doi.org/10.1029/2006JD007337)
- Xue F (2001) Interannual to interdecadal variation of East Asian summer monsoon and its association with the global atmospheric circulation and sea surface temperature. *Adv Atmos Sci* 18:567–575
- Yang MZ, Ding YH (2007) A study of the impact of south Indian Ocean dipole on the summer rainfall in China. *Chin J Atmos Sci* 31:685–694 (in Chinese)
- Yang S, Lau KM, Kim KM (2002) Variations of the East Asian jet stream and Asian-Pacific-American winter climate anomalies. *J Clim* 15:306–325
- Yim SY, Jhun JG, Yeh SW (2008) Decadal change in the relationship between east Asian–western North Pacific summer monsoons and ENSO in the mid-1990s. *Geophys Res Lett* 35:L20711. doi:[10.1029/2008GL035751](https://doi.org/10.1029/2008GL035751)
- Yim SY, Wang B, Kwon MH (2014) Interdecadal change of the controlling mechanisms for East Asian early summer rainfall variation around the mid-1990s. *Clim Dyn* 42:1325–1333. doi:[10.1007/s00382-013-1760-6](https://doi.org/10.1007/s00382-013-1760-6)
- Yu RC, Wang B, Zhou TJ (2004) Tropospheric cooling and summer monsoon weakening trend over East Asia. *Geophys Res Lett* 31:L22212. doi:[10.1029/2004GL021270](https://doi.org/10.1029/2004GL021270)
- Yuan F, Chen W (2013) Roles of the tropical convective activities over different regions in the earlier onset of the South China Sea summer monsoon after 1993. *Theor Appl Climatol* 113:175–185
- Zhai PM et al (2005) Trends in total precipitation and frequency of daily precipitation extremes over China. *J Clim* 18:1096–1108
- Zhou TJ et al (2009) Why the western pacific subtropical high has extended westward since the Late 1970s. *J Clim* 22:2199–2215
- Zhu J et al (2013) Decadal changes of Meiyu rainfall around 1991 and its relationship with two types of ENSO. *J Geophys Res Atmos* 118:9766–9777. doi:[10.1002/jgrd.50779](https://doi.org/10.1002/jgrd.50779)
- Zhu ZW, Li T, He JH (2014) Out-of-phase relationship between boreal spring and summer decadal rainfall changes in southern China. *J Clim* 27:1083–1099